SCIENTIFIC REPORTS

OPEN

SUBJECT AREAS:
HETEROGENEOUS CATALYSIS
CHEMICAL ENGINEERING
SUSTAINABILITY
MAGNETIC MATERIALS

Received
29 April 2013

Accepted
24 May 2013

Published
12 June 2013

Correspondence and requests for materials should be addressed to B.N.Z. (zongbn.ripp@sinopec.com) or M.H.Q. (mhqiao@fudan.edu.cn)

When Magnetic Catalyst Meets Magnetic Reactor: Etherification of FCC Light Gasoline as an Example

Meng Cheng[1], Wenhua Xie[1], Baoning Zong[1], Bo Sun[2] & Minghua Qiao[2]

[1]State Key Laboratory of Catalytic Materials and Reaction Engineering, Research Institute of Petroleum Processing, Beijing 100083, China, [2]Department of Chemistry and Shanghai Key Laboratory of Molecular Catalysis and Innovative Materials, Fudan University, Shanghai, 200433, China.

The application of elaborately designed magnetic catalysts has long been limited to ease their separation from the products only. In this paper, we for the first time employed a magnetic sulphonated poly(styrene-divinylbenzene) resin catalyst on a magnetically stabilized-bed (MSB) reactor to enhance the etherification of fluidized catalytic cracking (FCC) light gasoline, one of the most important reactions in petroleum refining industry. We demonstrated that the catalytic performance of the magnetic acid resin catalyst on the magnetic reactor is substantially enhanced as compared to its performance on a conventional fixed-bed reactor under otherwise identical operation conditions. The magnetic catalyst has the potential to be loaded and unloaded continuously on the magnetic reactor, which will greatly simplify the current complex industrial etherification processes.

In 2009, the gasoline production worldwide was approximately 22.1 million barrels per day[1], in which *ca.* 30% is FCC light gasoline. Olefins constitute 40–60% of FCC light gasoline, which are responsible for hazardous CO, ozone, and NO_x emissions[2]. However, among these olefins, about one half is tertiary olefins mainly with C_5 and C_6 carbon numbers (for details, see Supplementary Table S1 and related description online). Etherification of these C_5 and C_6 tertiary olefins with methanol to the desirable tertiary amyl methyl ether (TAME) and tertiary hexyl methyl ethers (THxMEs), respectively, will not only compensate for or add up to the octane number otherwise lost by olefin removal, but also boost the oxygen content in FCC light gasoline, as well as lower the Reid vapor pressure. As a consequence, etherification of tertiary olefins in FCC gasoline becomes one of the most important technologies in petroleum refinery[2]. Despite a variety of processes have been demonstrated, the acid resin-catalyzed etherification reaction is exclusively conducted on a fixed-bed reactor. Even for a newly developed process based on catalytic distillation, the acid resin catalyst still resides in the reactor in a fixed manner[3]. Since the acid resin catalyst in the fixed-bed reactor cannot be regenerated without interrupting the operation, rigorous impurity removal from FCC light gasoline and high stability of the catalyst are mandatory to ensure an acceptable working time of the catalyst. A typical flow diagram of the commercial etherification process is depicted in Supplementary Fig. S1a online. It is apparent that the commercial process is highly complicated, thus high capital and operation costs are demanded.

In recent years, the rapid development of versatile synthetic strategies for magnetic materials with controlled size, composition, and structure opens enormous possibilities for the preparation of heterogeneous or heterogenized homogeneous catalysts with magnetic properties[4–10]. Irrespective of these impressive advances, it is surprising that the application of the magnetic catalysts is very primitive, *i.e.*, their magnetic properties were only lavishly used to help in their separation[11–16]. The question arises and remains to be answered: is it possible to extract additional benefits from the magnetism of these elaborately designed magnetic catalysts? It is well documented that in heterogeneous catalysis, only in an adequate reactor can the merits of a catalyst be expressed perfectly[17]. So, is there such a reactor that can take full advantages of the magnetism of the magnetic catalysts?

More than three decades ago, Rosensweig in his pioneering work proposed the concept of MSB[18]. The MSB has three operation regimes with the increasing strength of the magnetic field: the scattered particulate regime, the chain regime, and the magnetic condensation regime[19]. When the MSB is operated in the chain regime, the particulates orient along the axial direction of the MSB in the chain form. The voidages between the chains are homogeneous, which is devoid of gas bypassing and solid backmixing, thus conducive to a good contact with the liquid or gas fluid[19]. Fine and friable particles can be used without penalties of high pressure drop[18]. So, the MSB

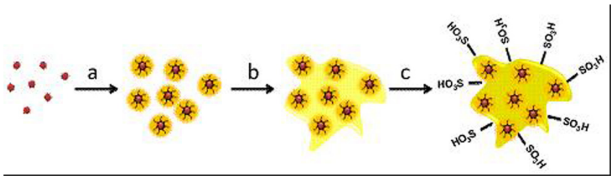

Figure 1 | Schematic illustration of the preparation procedures of the MS-PSD acid resin catalyst. (a) Modification of MNPs with UDA and coating with a dense PSD layer, (b) coating with porous PSD resin, (c) sulphonation with oleum.

operated in the chain regime offers a good chance for the development of a fascinating reactor especially suitable for heterogeneous catalysis. However, the application of this concept in catalysis has long been ignored[20], possibly due to the unavailability of the state-of-the-art magnetic catalysts at that age.

Herein, we prepared sulphonated poly(styrene-divinylbenzene) (PSD) resins with magnetism using magnetite nanoparticles (MNPs) as the magnetic core, and employed this magnetic acid resin catalyst (abbreviated as MS-PSD) on a laboratory-made MSB reactor (Supplementary Fig. S2 online) for etherification of FCC light gasoline, one of the most important reaction in petroleum refining industry affording oxygenates for gasoline blending[21–23]. We show that the catalytic performance of this magnetic acid resin catalyst on the MSB reactor is far superior to that on a conventional fixed-bed reactor under otherwise identical reaction conditions. Moreover, the MSB reactor is able to realize a continuous loading and unloading of the magnetic catalyst without interruption of the reaction, showing promise for etherifying FCC light gasoline in a simpler, greener, and more economic manner.

Results

The synthetic strategy for the MS-PSD acid resin catalyst was developed based on previous works[24–28], as illustrated in Fig. 1 (for details, see Supplementary Information online). In this strategy, a two-step suspension polymerization approach was employed to grow a dense PSD layer first to protect the MNPs from dissolution during sulphonation, followed by a porous coating to ensure a high acid capacity after sulphonation. Functionalization of the MNPs with organic acid, in the present case, undecylenic acid (UDA), enhances the dispersion of the MNPs in the hydrophobic phase during suspension polymerization[26,28]. Divinylbenzene tends to polymerize with the alkenyl groups on UDA-modified MNPs (UDA-MNPs) to improve the resistance of the MNPs to oleum. The wide-scan X-ray photoelectron spectrum (XPS, Fig. 2) of the MS-PSD acid resin reveals no signal from iron, confirming the robustness and integrity of the first PSD layer occluding the MNPs. In sharp contrast, signals from carbon, oxygen, and sulphur are clearly visible, reflecting the successful sulphonation of PSD.

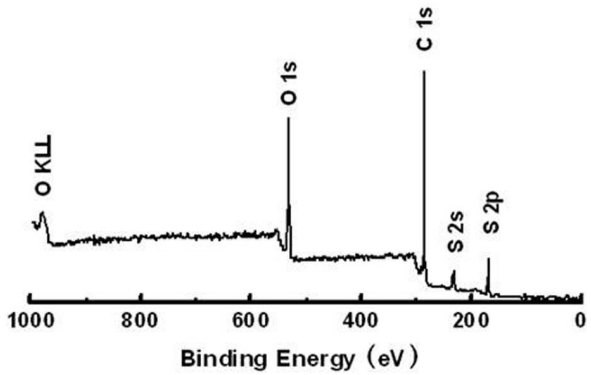

Figure 2 | Wide-scan XPS spectrum of the MS-PSD acid resin catalyst.

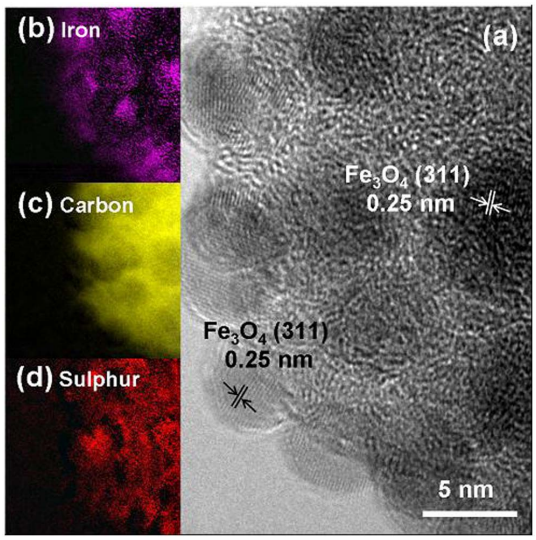

Figure 3 | (a) HRTEM image and elemental mapping images of (b) iron, (c) carbon, (d) sulphur of the MS-PSD acid resin catalyst.

The microstructure of the MS-PSD acid resin is better described as a dispersion of uniform MNPs in a sulphonated PSD matrix, as revealed by high-resolution transmission electron microscopy (HRTEM, Fig. 3a) of an intentionally crushed acid resin particle. Lattice fringes with interplanar spacing of 2.52 Å corresponding to the (3 1 1) planes of magnetite are visualized, which is consistent with the assignment based on powder X-ray diffraction (XRD, Supplementary Fig. S3 online). The average crystallite size of the MNPs calculated by the Scherrer equation and the (3 1 1) diffraction peak of magnetite is *ca.* 13 nm. Figures 3b–d display the elemental mapping images of iron, carbon, and sulphur corresponding to Fig. 3a. Carbon and sulphur are homogeneously distributed on the whole sample, while the distribution of iron nicely mimics the contours of the MNPs in Fig. 3a.

Figure 4 presents the magnetization curves of the UDA-MNPs, M-PSD, and MS-PSD at 298 K. All samples show negligible coercivity (H_c), which is characteristic for the superparamagnetic behavior of the MNPs. The specific saturation magnetization (M_s) of the UDA-MNPs (67.3 emu g^{-1}) is decreased to 20.8 emu g^{-1} after PSD coating, and decreased further to 12.3 emu g^{-1} after sulphonation. Based on the M_s of 72.2 emu g^{-1} for the starting MNPs, the weight percentages of MNPs of 93.2%, 28.8%, and 17.0% are estimated for UDA-MNPs, M-PSD, and MS-PSD, respectively. Thermogravimetric analyses

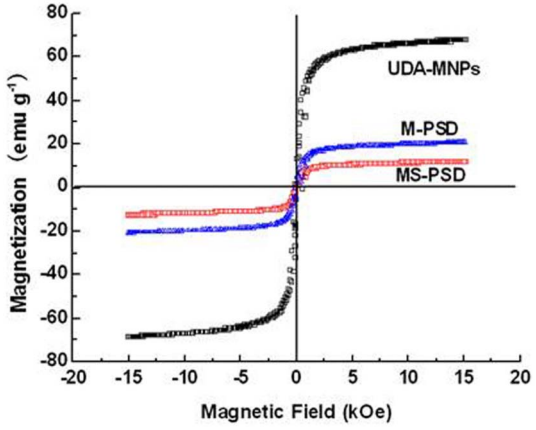

Figure 4 | Magnetization curves of the UDA-MNPs, M-PSD, and MS-PSD acid resin samples at 298 K.

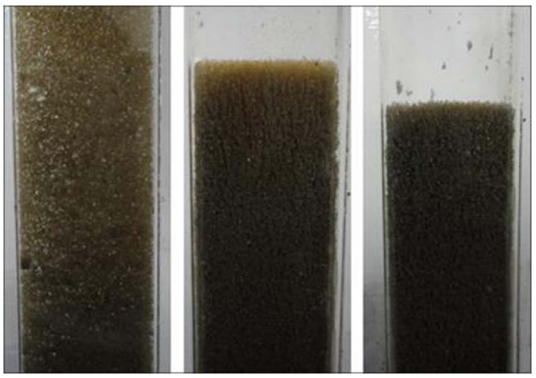

Figure 5 | Photographs for the MS-PSD acid resin catalysts in (a) the scattered particulate state, (b) the chain state, and (c) the magnetic condensation state. The strengths of the applied magnetic field are 0, 30, and 50 kA m^{-1} for (a), (b), and (c), respectively. To show these operation states, the tube accommodating the catalyst was made of transparent PMMA rather than stainless steel that is used for the reactor, and the fluid was changed to the colorless water rather than the yellowish FCC light gasoline for clarity. The liquid hourly space velocity (LHSV) was 1.0 h^{-1}, similar to the typical value for the etherification of FCC light gasoline.

(TGA, Supplementary Fig. S4 online) of the M-PSD and MS-PSD show that the contents of the MNPs are 28.6% and 17.7%, respectively, in agreement with the values deduced from magnetization measurements. It should be noted that although the dense PSD layer on MNPs cannot be distinguished in Fig. 3a due to the low electron density of carbon, another MS-PSD sample prepared only via the second polymerization step showed no magnetism, confirming the effectiveness of the first polymerization step in protecting the MNPs from acid dissolution.

The as-synthesized MS-PSD acid resin catalyst shows textural properties (Supplementary Table S2 online) similar to those of Amberlyst 15[22], a well-known commercial acid resin catalyst for the etherification of olefins[24,29]. The acid capacity (3.45 mmol g^{-1}) of the MS-PSD is lower than that of Amberlyst 15. But taking into account of the presence of ~17 wt% of MNPs in MS-PSD that does not contribute to the acid capacity and the first dense PSD layer that is resistant to sulphonation, such an acid capacity is expected. We verified that when the MNP-PSD only after the first polymerization step was subjected to the same sulphonation treatment, an acid capacity of ~0 is found. In another control experiment, when a sulphonated PSD (S-PSD) acid resin was synthesized in the way identical to that of MS-PSD but in the absence of the UDA-MNPs, the acid capacity of the S-PSD is 4.33 mmol g^{-1}, approaching to that of Amberlyst 15 (Supplementary Table S2 online).

Figure 5 presents the photographs of the MS-PSD magnetic acid resin catalyst in three operation regimes on the MSB reactor. The scattered particulate state (Fig. 5a), the chain state (Fig. 5b), and the condensation state (Fig. 5c) of the magnetic resin catalyst are clearly visible with the increment of the applied magnetic field of 0, 30, and 50 kA m^{-1}, respectively. Figure 6 compares the effects of the reaction parameters on the yield of TAME in the etherification of FCC light gasoline over the MS-PSD acid resin catalyst on the fixed-bed reactor and on the MSB reactor operated in the chain regime. It is revealed that the MS-PSD acid resin catalyst performs much better on the MSB reactor than on the fixed-bed reactor. Under the same etherification conditions, the yields of TAME on the MSB reactor always surpass those on the fixed-bed reactor. It is worth to note that even under very challenging reaction condition, *e.g.* the methanol/tertiary olefin ratio as low as 0.8 (Fig. 6a), the temperature as low as 338 K (Fig. 6b), the pressure as low as 0.6 MPa (Fig. 6c), or the liquid hourly space velocity (LHSV) as high as 2.5 h^{-1} (Fig. 6d), the yield of TAME is as high as 55.7%, 63.0%, 72.1%, or 61.7%, respectively. On the fixed-bed reactor, however, the corresponding value is only 33.8%,

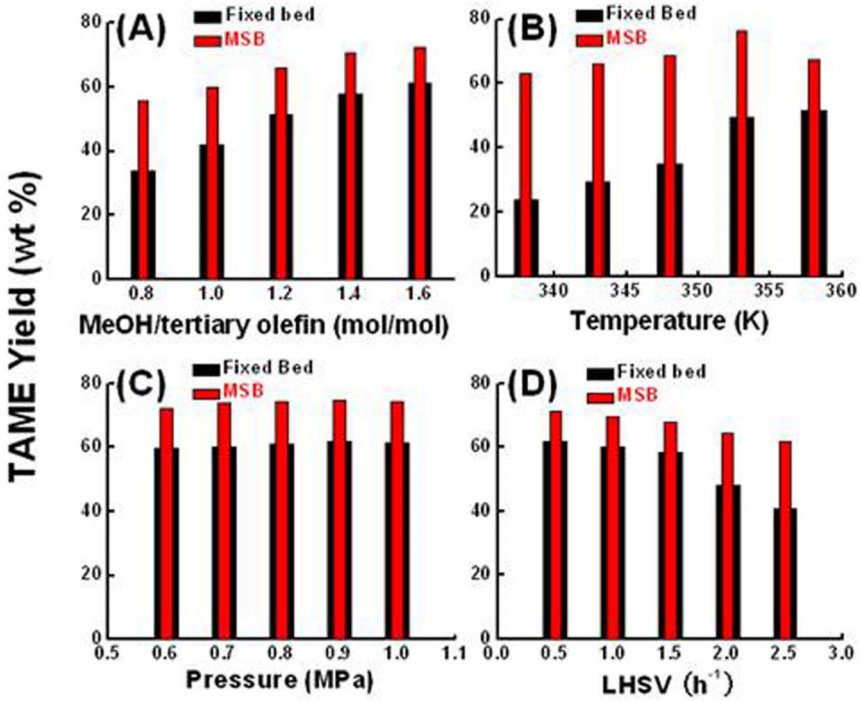

Figure 6 | The yields of TAME on the fixed-bed reactor and on the MSB reactor over the MS-PSD acid resin catalyst. (a) Effect of the feed ratio. Other reaction conditions: temperature of 353 K, pressure of 0.7 MPa, and LHSV of 1.0 h^{-1}. (b) Effect of the reaction temperature. Other reaction conditions: pressure of 0.7 MPa, MeOH/tertiary olefin ratio of 1.4, and LHSV of 1.0 h^{-1}. (c) Effect of the system pressure. Other reaction conditions: temperature of 353 K, MeOH/tertiary olefin ratio of 1.4, and LHSV of 1.0 h^{-1}. (d) Effect of the LHSV. Other reaction conditions: temperature of 353 K, pressure of 0.7 MPa, and MeOH/tertiary olefin ratio of 1.4. The magnetic field strength is 30 kA m^{-1} for the MSB reactor.

23.8%, 59.8%, or 40.6%. For reference, Rihko and Krause reported a TAME yield of 57.6% over an Amberlyst-type acid resin catalyst on the fixed-bed reactor, though that catalyst has a higher acid capacity (4.4 mmol g^{-1})[30] than our MS-PSD acid resin catalyst.

Moreover, the yield of TAME on the MSB reactor is less sensitive to variations in the reaction parameters. In the ranges of the methanol/tertiary olefin molar ratio of 0.8–1.6 (Fig. 6a), the temperature of 338–358 K (Fig. 6b), the pressure of 0.6–1.0 MPa (Fig. 6c), and the LHSV of 0.5–2.5 h^{-1} (Fig. 6d), the maximum variation in the yield of TAME does not exceed 31%. On the fixed-bed reactor, the corresponding change is in a much broader range of 3–117%. Thus, when using the MSB reactor for the etherification of FCC light gasoline, the control of the reaction condition becomes a less demanding task, which renders the operation with exceptional simplicity. Moreover, the composition of the FCC light gasoline depends on the source of the crude oil, the type of the FCC catalyst, and the FCC reaction condition, and is thus widely variable[2]. Therefore, etherification of FCC light gasoline on the MSB reactor offers an appealing opportunity for processing FCC light gasoline of different origins without imparting additional operation severity to the purification steps, as the broad operation flexibility of the MSB reactor can readily offset such variations. A similar positive effect of the MSB reactor on the yield of THxMEs from the etherification of C_6 tertiary olefins in FCC light gasoline can be found in Supplementary Fig. S5 online.

Supplementary Table S3 online lists the composition of the etherified FCC light gasoline on the fixed-bed reactor (LHSV: 0.5 h^{-1}) and on the MSB reactor (LHSV: 1.0 h^{-1}) under reaction conditions of temperature of 353 K and pressure of 0.7 MPa. Even though the LHSV on the MSB reactor is two folds of that on the fixed-bed reactor, there are still less residual unconverted C_5 and C_6 tertiary olefins and more TAME and THxMEs on the MSB reactor, manifesting again the higher efficiency of the MSB reactor in etherifying FCC light gasoline.

Discussion

The MSB has the merits of low pressure drop, absence of particle mixing, and high interphase heat and mass transportation[19], which can account for the superiority of the MSB reactor in etherifying FCC light gasoline. Furthermore, by adjusting the strength of the applied magnetic field, the magnetic particles are able to move out of the MSB under control[31], allowing for continuous loading and unloading of the magnetic particles. Therefore, catalytic activity loss caused by impurity accumulation can be circumvented by on-site replenish of the catalyst, which further alleviates the stringent demands for the purification steps and the lifetime of the acid resin catalyst. A more compact etherification process based solely on a dual-MSB reactor set-up is envisaged, as depicted in Supplementary Fig. S1b online. In this innovative process, one MSB reactor is used for etherifying FCC light gasoline without purification, the other is for reactivating the spent catalyst and supplying the reactivated or fresh catalyst to the first reactor. This design shows the prospect for etherifying FCC light gasoline in a much simpler and more economic way. We identified in a preliminary experiment that the spent MS-PSD magnetic acid resin catalyst with *ca.* 45% of its original activity can be recovered to *ca.* 80% of its original activity by washing with methanol followed by 1.0 M HCl, which is easily integrated to this novel on-site reactivation process.

We have successfully demonstrated that the right place for a magnetic catalyst is the magnetic reactor. On the MSB reactor, the magnetic acid resin catalyst not only works more efficiently in etherifying FCC light gasoline, but also becomes more resistant to fluctuations in reaction conditions than on the fixed-bed reactor. Moreover, the magnetic catalyst has the potential to be replenished on-site in a dual-MSB reactor set-up rendering an uninterrupted process, which adds unprecedented operation simplicity to the etherification process. The "magnetic catalyst-on-magnetic reactor" strategy can find wide applications in many energy- and environment-important reactions, especially in cracking, dehydrogenation, and reforming that are plagued by fast catalyst deactivation. In this connection, this new strategy envisages significant changes in the economic and environmental impacts of chemical production processes, and will greatly stimulate the design of new synthetic approaches for magnetic catalytic materials.

Methods

The surface species of the MS-PSD acid resin catalyst were detected by XPS (Perkin Elmer PHI Quantera SXM). The spectrum was recorded with monochromatized Al Kα line ($h\nu$ = 1,486.6 eV) as the excitation source. The sensitivity was 3 MCPS. TEM characterization and elemental mapping were conducted on an FEI TECNAI F20 G2 electron microscope operated at 200 kV, to which a Gatan GIF 2001 spectrometer was attached. The energy filter images were recorded under the EFTEM mode. The width of the energy filter slit was 10 eV, the GIF incidence aperture was 0.6 mm, and the 3-window method was applied during elemental mapping collection. The magnetization curves were measured on a vibrating sample magnetometer (VSM, JDM-13, Jilin Univ.) at room temperature.

The construction of the MSB reactor is described as follows. A stainless steel tube of 9 mm i.d. and 700 mm long was surrounded by three identical DC-powered annular coils with each homogeneously wounded by 400 cycles of tabular copper wires. The i.d. and o.d. of the coils are 65 and 160 mm, respectively, and the height is 60 mm. The distance between the centers of two neighboring coils is 65 mm. A uniform axial magnetic field of up to 50.0 kA m^{-1} can be generated by adjusting the current passing through the copper coils. The catalyst loading was 2.5 g for each catalytic run. Before feeding anhydrous methanol (A.R., Beijing Chemical) and FCC light gasoline (Beijing Yanshan Petrochem.), the reactor system was purged with N_2 at 10.0 mL min^{-1} using an electronic mass flow controller (D08-8B/ZM, Qixing Huachuang Co., Ltd.) for 1 h at room temperature, and then pressurized with N_2. The feedstocks were then pumped into the reactor at a desired flow rate via two high pressure pumps (NP-KX-110, Nihon Seimitsu Kagaku Co., Ltd.). The effluents were condensed and analyzed gas chromatographically. Etherification of FCC light gasoline with methanol on this magnetic acid resin catalyst was also evaluated on a fixed-bed reactor. The construction of the fixed-bed reactor is the same as that of the MSB reactor, except for the absence of the electromagnetic coils.

1. Tian, C. R. China's oil import and export in 2009. *Int. Petro. Econ. (in Chinese)* **18**, 4–13 (2010).
2. Pescarollo, E., Trotta, R. & Sarathy, P. R. Etherify light gasolines. *Hydrocarbon Process.* **72**, 53–60 (1993).
3. Harmsen, G. J. Reactive distillation: The front-runner of industrial process intensification: A full review of commercial applications, research, scale-up, design and operation. *hem. Eng. Process.* **46**, 774–780 (2007).
4. Sun, S. H., Murray, C. B., Weller, D., Folks, L. & Moser, A. Monodisperse FePt nanoparticles and ferromagnetic FePt nanocrystal superlattices. *Science* **287**, 1989–1992 (2000).
5. Redl, F. X., Cho, K. S., Murray, C. B. & O'Brien, S. Three-dimensional binary superlattices of magnetic nanocrystals and semiconductor quantum dots. *Nature* **423**, 968–971 (2003).
6. Mao, C. B. *et al.* Virus-based toolkit for the directed synthesis of magnetic and semiconducting nanowires. *Science* **303**, 213–217 (2004).
7. Yavuz, C. T. *et al.* Low-field magnetic separation of monodisperse Fe_3O_4 nanocrystals. *Science* **314**, 964–967 (2006).
8. Lu, A. H., Salabas, E. L. & Schüth, F. Magnetic Nanoparticles: Synthesis, Protection, Functionalization, and Application. *Angew. Chem. Int. Ed.* **46**, 1222–1244 (2007).
9. Latham, A. H. & Williams, M. E. Controlling transport and chemical functionality of magnetic nanoparticles. *Acc. Chem. Res.* **41**, 411–420 (2008).
10. Shylesh, S., Schünemann, V. & Thiel, W. R. Magnetically separable nanocatalysts: Bridges between homogeneous and heterogeneous catalysis. *Angew. Chem. Int. Ed.* **49**, 3428–3459 (2010).
11. Tsang, S. C. E., Caps, V., Paraskevas, I., Chadwick, D. & Thompsett, D. Magnetically separable, carbon-supported nanocatalysts for the manufacture of fine chemicals. *Angew. Chem. Int. Ed.* **43**, 5645–5649 (2004).
12. Abu-Reziq, R., Alper, H., Wang, D. S. & Post, M. L. Metal supported on dendronized magnetic nanoparticles: Highly selective hydroformylation catalysis. *J. Am. Soc. Chem.* **128**, 5279–5282 (2006).
13. Panella, B., Vargas, A. & Baiker, A. Magnetically separable Pt catalyst for asymmetric hydrogenation. *J. Catal.* **261**, 88–93 (2009).
14. Jin, M. J. & Lee, D. H. A practical heterogeneous catalyst for the Suzuki, Sonogashira, and Stille coupling reactions of unreactive aryl chlorides. *Angew. Chem. Int. Ed.* **49**, 1119–1122 (2010).
15. Polshettiwar, V. *et al.* Magnetically recoverable nanocatalysts. *Chem. Rev.* **111**, 3036–3075 (2011).
16. Lai, D. M., Deng, L., Guo, Q. X. & Fu, Y. Hydrolysis of biomass by magnetic solid acid. *Energy Enivron. Sci.* **4**, 3552–3557 (2012).

17. Moulijn, J. A., van Diepen, A. E. & Kapteijn, F. In *Handbook of Heterogeneous Catalysis* (ed Ertl, G., Knözinger, H., Schüth, F. & Weitkamp, J.) Chap. 7 (Wiley-VCH: Weinheim, 2008).
18. Rosensweig, R. E. Fluidization: hydrodynamic stabilization with a magnetic field. *Science* **204**, 57–60 (1979).
19. Zong, B. N. Intensification catalytic reaction by integration of magnetic catalyst and magnetically stabilized bed reactor or magnetic separator. *Catal. Surv. Asia* **11**, 87–94 (2007).
20. Pan, Z. Y. *et al*. Integration of magnetically stabilized bed and amorphous nickel alloy catalyst for CO methanation. *Chem. Eng. Sci.* **62**, 2712–2717 (2007).
21. Wyczesany, A. Chemical equilibria in the process of etherification of light FCC gasoline with methanol. *Ind. Eng. Chem. Res.* **34**, 1320–1326 (1995).
22. Girolamo, M. D. *et al*. Liquid-phase etherification/dimerization of isobutene over sulfonic acid resins. *Ind. Eng. Chem. Res.* **36**, 4452–4458 (1997).
23. Girolamo, M. D. & Tagliabue, L. MTBE and alkylate co-production: Fundamentals and operating experience. *Catal. Today* **52**, 307–319 (1999).
24. Kunin, R., Meitzner, E. & Bortnick, N. Macroreticular ion exchange resins. *J. Am. Chem. Soc.* **84**, 305–306 (1962).
25. Martin, C., Ramirez, L. & Cuellar, J. Stainless steel microbeads coated with sulfonated polystyrene-co-divinylbenzene. *Surf. Coating Technol.* **165**, 58–64 (2003).
26. Lee, Y., Rho, J. & Jung, B. Preparation of magnetic ion-exchange resins by the suspension polymerization of styrene with magnetite. *J. Appl. Polym. Sci.* **89**, 2058–2067 (2003).
27. Yang, C. L. *et al*. Preparation of magnetic polystyrene microspheres with a narrow size distribution. *AIChE J.* **51**, 2011–2015 (2005).
28. Feyen, M., Weidenthaler, C., Schüth, F. & Lu, A. H. Synthesis of structurally stable colloidal composites as magnetically recyclable acid catalysts. *Chem. Mater.* **22**, 2955–2961 (2010).
29. Chakrabarti, A. & Sharma, M. M. Cationic ion exchange resins as catalyst. *React. Polym.* **20**, 1–2 (1993).
30. Rihko, L. K. & Krause, A. O. I. Etherification of FCC light gasoline with methanol. *Ind. Eng. Chem. Res.* **35**, 2500–2507 (1996).
31. Cocker, T. M., Fee, C. J. & Evans, R. A. Preparation of magnetically susceptible polyacrylamide/magnetite beads for use in magnetically stabilized fluidized bed chromatography. *Biotechnol. Bioeng.* **53**, 79–87 (1997).

Acknowledgements

This work was supported by the National Basic Research Program of China (2012CB224800), the Science & Technology Commission of Shanghai Municipality (10JC1401800, 08DZ2270500), the NSF of China (21073043), and the Program of New Century Excellent Talents (NCET-08-0126).

Author contributions

B.N.Z. conceived and designed the experiments. M.C. and W.H.X. carried out synthesis, characterization and etherification experiments. B.S. performed HRTEM analysis. M.H.Q. participated in the discussion and contributed to the writing and revision of the manuscript.

Additional information

Supplementary information accompanies this paper at http://www.nature.com/scientificreports

Competing financial interests: The authors declare no competing financial interests.

How to cite this article: Cheng, M., Xie, W., Zong, B., Sun, B. & Qiao, M. When Magnetic Catalyst Meets Magnetic Reactor: Etherification of FCC Light Gasoline as an Example. *Sci. Rep.* **3**, 1973; DOI:10.1038/srep01973 (2013).